Improved determination of rigid plate motion by incorporating intraplate deformation models.

H.-P. Plag (1), C. Kreemer (1), and H. P. Kierulf (2)

(1) Nevada Bureau of Mines and Geology and Seismological Laboratory, University of Nevada, Reno, Mailstop 178, Reno, NV 89557, USA, email: hpplag@unr.edu./kreemer@unr.edu

(2) Norwegian Mapping Authority, 3507 Honefoss, Norway, email: halfdan.kierulf@statkart.no.

Introduction

For many scientific and non-scientific applications, positions determined at different epochs need to be intercompared or positions need to be referred to a common epoch. For that, a plate motion model is required that has a high accuracy; better than 1 mm/yr for the most demanding applications. Over the last 15 years, various plate motion models have been derived. Most of these models describe the global horizontal motions by a set of rigid plates distributed over the Earth's spherical surface. For each plate, the motion is fully determined by a 3-d rotation vector which fixes the corresponding Euler pole. These vectors are determined in a least squares fit of the predicted angular velocity field of the plates to observed geodetic velocities. For most plates, the uncertainty in the rotation vector is still large and is mainly the result of the lack of having a set of well-distributed velocity measurements on the plate. Moreover, these vectors turn out to be dependent on the pre-selection of observed velocities used in the data fit. For some plates, site selection for the data fit is dominated by the presence of well known, but possibly not well modelled, intraplate deformation. Proper modelling of this deformation could yield much better spatial data coverage and would thus enhance the stability and accuracy of the rotation vectors.

Methodology

Any observed velocity field over a tectonic plate can be represented as a sum of a rigid body rotation and a velocity field due to intraplate deformation. In most models of plate motion, the part of the velocity field $\vec{V}$ that is due to rigid plate motion is represented for each plate k by the vector product of a plate specific constant rotation vector $\vec{\omega}_k$ and the position vector $\vec{X}$, i.e.

$$\vec{V}_k(\vec{X}) = \vec{\omega}_k \times \vec{X} \quad (1)$$

In most studies, the rotation vectors are determined through a least squares fit of this equation to observed velocities. Plag et al. (2002) suggested to extend this standard approach by including known intra-plate deformations in eq. (1) leading to

$$\vec{V}(\vec{X}) = \vec{\omega} \times \vec{X} + \sum_{i=1}^{n} \vec{G}_i(\vec{X}) \quad (2)$$

where G_i are the velocities predicted for the $i-$th processes. One of these processes acting on a regional to global scale, for which sufficiently accurate models are available, is the post-glacial rebound signal (PGS). Kierulf et al. (2003) estimated an improved rotation vector for the Eurasian plate by fitting a modified form of eq. (2) to the observed ITRF velocity field. However, their estimate was based on one PGS predictions only, thus not allowing to study the sensitivity of the approach to the uncertainty in the model predictions.

Here, we study the effect of PGS on the resulting rotation vectors by including the present-day velocities predicted by various rebound models in the least squares fit for most major plates and for two different observed velocity fields. We perform our analysis in a geocentric coordinate system and we do not consider observed or predicted vertical rates. We incorporate the velocities from the rebound models by taking into account a possible displacement vector rate $\vec{\Delta}$ of the origin of the reference frame in which the PGS predictions $\vec{V}^{\mathrm{P}}(\vec{X})$ are presented, and also by considering a possible scaling γ of the predicted rates. We perform the analysis for each plate separately. Thus, the velocity field of plate k is modeled by

$$\vec{V}_k(\vec{X}) = (\vec{\omega}_k \times \vec{X}) + \vec{\Delta}_k + \gamma_k \vec{V}^{\mathrm{P}}(\vec{X}) \quad (3)$$

For each plate with more than 3 stations we solve for $\vec{\omega}$, $\vec{\Delta}$, and γ. We compare $\vec{\omega}$ with the angular velocity obtained for a model in which only a rigid body rotations was determined. We also determine through an F-test the improvement of the fit of eq. (3) to the observed velocities due to the inclusion of the PGS compared to a fit without PGS.

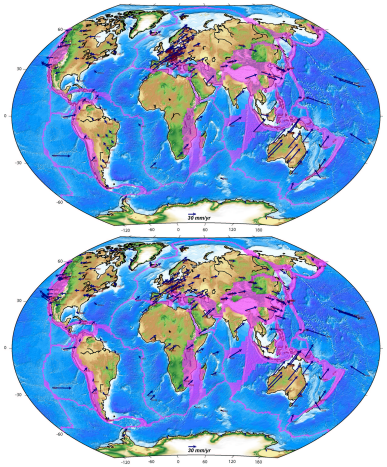

Figure 1: Observed velocity fields. *Upper panel: Velocity field determined from the gpsvel analysis Lavallée et al. (2001). Lower panel: velocity field for ITRF2000 (Altamimi et al., 2002).*

Observed velocity field

We have used two different observed velocity fields (Figure 1). The GPSVEL solution (176 solutions) is an update of the solution presented by Lavallée et al. (2001). It is derived from a free-network combination of weekly station coordinates from 7 global IGS analysis centers and 3 regional associate analysis centers (Australia, Europe, and South America). The 'Altamimi' solution (199 stations) is from an update of Altamimi et al. (2002). It is derived from a combination of gloval GPS, VLBI, SLR, DORIS and LLR solutions and provided by Altamimi (2005, personal communication).

Post-glacial rebound models.

Table 1: Post-glacial rebound models used in the study.

No.	Model	Upper Mantle viscosity 10^{20} Pas	Lower Mantle viscosity 10^{20} Pas	Lithosphere thickness km	Ice model
M1	Mitrovoca	10.0	50.	120	ICE-3G
M2	Peltier 4	3.2 to 7.1	9.0 to 39.2	90	ICE-5G
M3	Peltier 2	3.7 to 7.7	12.7 to 39.2	90	ICE-5G

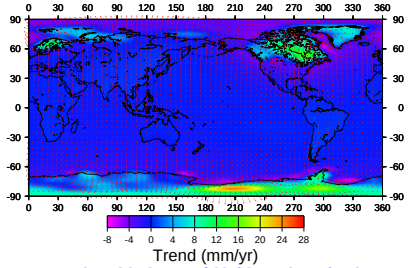

Figure 2: Present-day 3-d displacement field of the Earth's surface due to post-glacial rebound. *The predictions are for model M1 in Table 1. Arrows indicate direction and magnitude of horizontal displacements, colours the magnitude of the vertical component.*

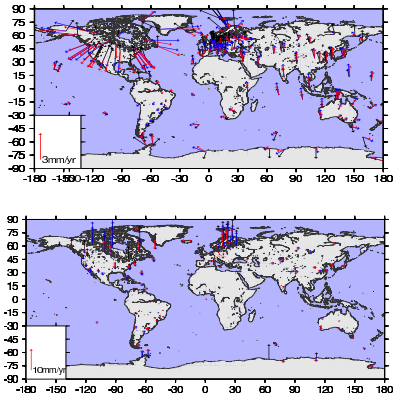

Figure 3: Predicition of pgs velocities at the observation points. *The predictions are compared for the three models and for all points where velocities are given. Black: M1, blue: M2, red: M3. Upper panel is for the horizontal components, lower panel for the vertical component.*

Predictions of the PGS are available for three models (Table 1). For all three models, the Earth model is spherically symmetric with the elastic parameters according to PREM. M1 has a two-layer viscosity model and uses the ice model ICE-3G (Milne et al., 1999). Models M2 and M3 have radius dependent viscosity structure and use the ice model ICE-5G (Peltier, 2004).

The global velocity field for M1 is shown in Figure 2. In Figure 3, we compare the predictions for the three models at the sampling points of the observed velocity fields shown in Figure 1. Intermodel difference are of the order of 0.5 mm/yr in the horizontal component and reach more than 5 mm/yr for the vertical.

References

Altamimi, Z., Sillard, P., & Boucher, C., 2002. A new release of the International Terrestrial Reference Frame for earth science applications, *J. Geophys. Res.*, **107**, 2214, doi: 10.1029/2001JB000561.

Kierulf, H. P., Plag, H.-P., & Kristiansen, O., 2003. Towards the true rotation of a rigid Eurasia, in *EUREF Publication No. 12*, edited by J. A. Torres & H. Hornik, no. 29 in Mitteilungen des Bundesamtes für Kartografie und Geodäsie, pp. 118–124, Verlag des Bundesamtes für Kartographie und Geodäsie, Frankfurt am Main.

Lavallée, D., Blewitt, G., Clarke, P. J., Nurutdinov, K., Holt, W. E., Kreemer, C., Meertens, C. M., Shiver, W. S., Stein, S., Zerbini, S., Bastos, L., & Kahle, H.-G., 2001. GPSVEL project: towards a dense global GPS velocity field, Presented at the IAG Scientific Assembly, Budapest, 2001.

Results

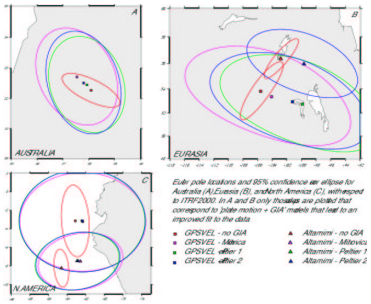

Figure 4: Geographical locations of the rotation poles for major plates.

Table 2: Improvement of models. *The χ^2 values in the headers are for the solution without PGS. N is the number of velocity samples. The maximum difference in velocity (Max. V) due to the inclusion of the PGS is given for fits with significant improvements, only.*

Australia	gpsvel		Altamimi	
	$\chi^2 = 1.247$	$N = 13$	$\chi^2 = 0.788$	$N = 13$
Model	Max. V	χ^2	Max. V	χ^2
M1		1.171	0.65	0.343
M2		1.056	1.73	0.252
M3		1.122	1.33	0.272
Eurasia	**gpsvel**		**Altamimi**	
	$\chi^2 = 0.572$	$N = 58$	$\chi^2 = 1.140$	$N = 41$
Model	Max. V	χ^2	Max. V	χ^2
M1	0.89	0.530		1.095
M2	0.35	0.517		1.110
M3	0.29	0.524	0.70	1.054
North America	**gpsvel**		**Altamimi**	
	$\chi^2 = 0.473$	$N = 20$	$\chi^2 = 1.630$	$N = 31$
Model	Max. V	χ^2	Max. V	χ^2
M1		0.504		1.658
M2		0.516		1.688
M3		0.510		1.683

Discussion of fits

Inclusion of PGS in the model equation results in significant improvements only for the Eurasian and Australian plates (Table 2). For the Eurasian plate, the improvement is only significant for the GPSVEL solution, which has a large number of stations in Europe (EUREF) and only a few in Siberia, whereas the Altamimi solution is more uniformly distributed over the whole Eurasian plate. This may indicate that the PGS models are representative for Europe but less for the other geopgraphical regions of the Eurasian plates. Poor model predictions for e.g. Siberia would compromise the fit for the Altamimi solution while leaving the one for the GPSVEL solution relatively unaffected.

For the Australian plate, which is in the far-field of the PGS, the spatial variations of the PGS are small compared to e.g. Africa. Thus, it may be easier to scale and translate the PGS predictions such that they can be used to seperate plate motions from an apparent PGS pattern. For the GPSVEL solution, where we do not get a significant improvement, there are two stations with rather large misfit, and these two stations may compromise the overall fit. However, it is worth to note that the scaling factor for Australia turns out to be consistently negative for all models (Table 3). This seems to indicate that either the PGS predictions for Australia are wrong or another geodynamic process is masking the finger-print of the PGS on this plate.

For North America, inclusion of the PGS in fact leads to a degradation of the fit (i.e. a χ^2 larger than for the solution without PGS). Moreover, the values for γ and $\vec{\Delta}$ are close to zero. There seems to be no combination of the scaling factor and the offset that would result in an improvement of the fit. Thus, the PGS predictions are not seen by the observed velocity field. However, for the northern part of the plate this may not be correct. Unlike Europe, the North American plate covers both the near-field and the far-field of the PGS and the near-field may in fact be better modeled.

It is interesting to note that for all three plates considered here the translation is small (almost all < 1.2 mm/yr, Table 3). The scaling factor shows significant variations between the PGS models.

Conclusions

For the Eurasian plate, the near-field PGS is easily identified in the observed velocity field and inclusion of this signal leads to a significant improvement of the Euler pole (Figure 4). For the North America plate, the geographical region representing the near-field needs to be considered separately to confirm this positive result for this plate, too. For the far-field regions, inclusion of the PGS does not result in an improvement of the fit. This may be due to the PGS predictions being less accurate in the far field. One reason for that could be the spherical symmetry of the rebound models, which cannot take into account the significant lateral heterogeneities in the viscosity of the Earth' mantle, which are e.g. present under the North American plate. Another reason maybe other geodynamic processes introducing larger intra-plate deformations than the PGS and thus masking this signal.

Further improvements are expected from addressing different regions of the individual plates separately, thus accounting for the effect of potential effects of lateral heterogeneities on the PGS prediction and also different geodynamic regims. Assuming that the PGS models are predicting the actual PGS, then a global fit solving for global values of $delta$ and $gamma$ would allow to determine the PGS model leading to the best fit. Another important step is to extend the analysis to also include the vertical component of the velocity field.

Milne, G. A., Mitrovica, J. X., & Davis, J. L., 1999. Near-field hydro-isostasy: the implementation of a revised sea-level equation, *Geophys. J. Int.*, **139**, 464–482.

Peltier, W. R., 2004. Global glacial isostasy and the surface of the ice-age Earth: The ICE-5G(VM2) model and GRACE, journal =Ann. Rev. Earth Planet Sci., volume =32, pages =111-149.

Plag, H.-P., Nørbech, T., & Kristiansen, O., 2002. Effects of intraplate deformations on fixing regional reference frames, in *EUREF Publication No. 10*, edited by J. A. Torres & H. Hornik, no. 23 in Mitteilungen des Bundesamtes für Kartografie und Geodäsie, pp. 118–124, Verlag des Bundesamtes für Kartographie und Geodäsie, Frankfurt am Main.

Acknowledgements

The authors would like to thank W.R. Peltier and J. Mitrovica for making their PGS predictions available. The authors are also grateful to Z. Altamimi, G. Blewitt and D. Lavallée for the provision of the velocity data. The work at UNR was funded by grants from NASA Solid Earth and NASA Interdisplinary Science.

Table 3: Offsets and scaling factors for pgs model predictions. *For each fit, the upper line gives the estimated components of $\vec{\Delta}$ and γ and the lower line gives the respective standard deviations. The components of $\vec{\Delta}$ are given in mm/yr and γ is dimensionless.*

	dx δdx	dy δdy	dz δdz	γ $\delta\gamma$
Australia				
GPSvel				
M1	0.0405	0.0666	-0.3527	-1.6168
	1.2839	0.9603	1.7089	0.7615
M2	0.0828	-0.0162	-0.2860	-1.8036
	1.2810	0.9615	1.7039	0.6767
M3	0.0423	0.0105	-0.2675	-1.2658
	1.2807	0.9614	1.7041	0.5164
Altamimi				
M1 *	-0.2721	0.1433	0.3229	-1.5458
	0.7314	0.5832	1.0658	0.5024
M2 *	-0.1846	-0.0061	0.1683	-1.4042
	0.7325	0.5852	1.0648	0.4158
M3 *	-0.2297	0.0162	0.2220	-1.0570
	0.7318	0.5847	1.0648	0.3188
Eurasia				
	dx δdx	dy δdy	dz δdz	γ $\delta\gamma$
GPSvel				
M1 *	0.2260	0.7766	-0.3107	0.3909
	0.7325	1.1906	0.6306	0.1680
M2 *	0.5330	1.4134	-0.6228	0.8200
	0.7362	1.1937	0.6354	0.3352
M3 *	0.3970	1.1540	-0.4806	0.5864
	0.7319	1.1854	0.6300	0.2463
Altamimi				
M1	0.2144	0.5011	-0.3210	0.3539
	0.4266	0.7943	0.3829	0.1427
M2	0.2469	0.7638	-0.3599	0.6461
	0.4277	0.7961	0.3844	0.2884
M3 *	0.2433	0.7255	-0.3597	0.6843
	0.4269	0.7940	0.3834	0.2192
North America				
	dx δdx	dy δdy	dz δdz	γ $\delta\gamma$
GPSvel				
M1	-0.0041	0.1459	0.1701	0.1547
	1.0146	0.8233	0.7102	0.2448
M2	-0.0352	0.1651	0.2711	0.0503
	1.0146	0.8240	0.7161	0.1155
M3	-0.0387	0.1752	0.2831	0.0552
	1.0146	0.8246	0.7158	0.1015
Altamimi				
M1	-0.3366	0.3755	0.4180	0.1786
	0.5424	0.4383	0.4952	0.1487
M2	-0.3813	0.4138	0.5402	0.0816
	0.5414	0.4399	0.5004	0.0696
M3	-0.3735	0.4232	0.5435	0.0745
	0.5414	0.4405	0.5005	0.0621

References

Altamimi, Z., Sillard, P., & Boucher, C., 2002. A new release of the International Terrestrial Reference Frame for earth science applications, *J. Geophys. Res.*, **107**, 2214, doi: 10.1029/2001JB000561.

Kierulf, H. P., Plag, H.-P., & Kristiansen, O., 2003. Towards the true rotation of a rigid Eurasia, in *EUREF Publication No. 12*, edited by J. A. Torres & H. Hornik, no. 29 in Mitteilungen des Bundesamtes für Kartografie und Geodäsie, pp. 118–124, Verlag des Bundesamtes für Kartographie und Geodäsie, Frankfurt am Main.

Lavallée, D., Blewitt, G., Clarke, P. J., Nurutdinov, K., Holt, W. E., Kreemer, C., Meertens, C. M., Shiver, W. S., Stein, S., Zerbini, S., Bastos, L., & Kahle, H.-G., 2001. GPSVEL project: towards a dense global GPS velocity field, Presented at the IAG Scientific Assembly, Budapest, 2001.

Milne, G. A., Mitrovica, J. X., & Davis, J. L., 1999. Near-field hydro-isostasy: the implementation of a revised sea-level equation, *Geophys. J. Int.*, **139**, 464–482.

Peltier, W. R., 2004. Global glacial isostasy and the surface of the ice-age Earth: The ICE-5G(VM2) model and GRACE, journal =Ann. Rev. Earth Planet Sci., volume =32, pages =111-149.

Plag, H.-P., Nørbech, T., & Kristiansen, O., 2002. Effects of intraplate deformations on fixing regional reference frames, in *EUREF Publication No. 10*, edited by J. A. Torres & H. Hornik, no. 23 in Mitteilungen des Bundesamtes für Kartografie und Geodäsie, pp. 118–124, Verlag des Bundesamtes für Kartographie und Geodäsie, Frankfurt am Main.